

Continuous flow synthesis of *N*-(2-aminophenyl) benzamide with high selectivity and its kinetic study in a microreactor

Qilin Xu¹, Hongmiao Yao¹, Huachun Fan¹, Zhikuo Wang¹, Na Li¹, Jiadi Zhou¹, Zhiquan Yu¹, and Weike Su¹

¹Zhejiang University of Technology

September 10, 2020

Abstract

The monobenzoylation of *o*-phenylenediamines (**DA**) is an important process to synthesis *N*-(2-aminophenyl) benzamide (**MP**), which is a key intermediate of many active compounds. But the monoacylation is difficult to control because this process is a kind of consecutive reaction system and the two amine groups located in a similar chemical environment. To understand the effects of reaction parameters on the selectivity and further optimize operating conditions, a microreactor platform was developed to evaluate the kinetics of the acylation reaction of **DA** and benzoic anhydride (**BH**). A kinetic model was established, and the reaction order of each reactant, the values of kinetic constants, pre-exponential factors and activation energies were determined. Validation experiments showed the model is in good agreement with the experimental results. The model simulation indicated that high reaction temperature and molar ratio of **DA** and **BH** is necessary to improve reaction efficiency and selectivity.

Abstract

The monobenzoylation of *o*-phenylenediamines (**DA**) is an important process to synthesis *N*-(2-aminophenyl) benzamide (**MP**), which is a key intermediate of many active compounds. But the monoacylation is difficult to control because this process is a kind of consecutive reaction system and the two amine groups located in a similar chemical environment. To understand the effects of reaction parameters on the selectivity and further optimize operating conditions, a microreactor platform was developed to evaluate the kinetics of the acylation reaction of **DA** and benzoic anhydride (**BH**). A kinetic model was established, and the reaction order of each reactant, the values of kinetic constants, pre-exponential factors and activation energies were determined. Validation experiments showed the model is in good agreement with the experimental results. The model simulation indicated that high reaction temperature and molar ratio of **DA** and **BH** is necessary to improve reaction efficiency and selectivity.

Keywords: monobenzoylation; *N*-(2-aminophenyl) benzamide; microreactor; continuous flow; kinetics study

Introduction

N-(2-aminophenyl) benzamide (**MP**), the monobenzoylation product of *o*-phenylenediamines (**DA**), is a valuable building blocks that have been utilized for construction of a variety of targets such as oligoamide foldamers,^{1,2} chemosensors³ and urolithins B⁴ and many pharmaceutically active agents.^{5,6} Obviously, the synthesis of **MP** from **DA** requires controlled acylation of one amino group while keeping the other group free, which is a kind of classic consecutive reaction system. The monoacylation selectivity of **DA** is rather difficult to control because the two amine groups are located in a similar chemical environment. For this kind of symmetrical diamines, many researchers have been committed to develop a novel catalysts⁷⁻¹¹ or specific acylation reagents¹²⁻¹⁵ to improve the monoacylation selectivity. However, this kind of method suffers from their own limitation, the catalysts or acylation reagents are usually rather complicated and expensive, which hinder its industrial application. *N*-BOC mono-protection of the diamine followed by acylation and

deprotection is the last resort, because this strategy is waste intensive and introduces extra steps to the synthesis, along with the need for additional purifications. In contrast, the direct condensation of **DA** with simply acylation reagent (acid chloride or acid anhydride) without any addition agent is the most desirable monoacylation method. Meanwhile, it is widely known that reaction regioselectivity is also controlled by the type of reactor and reaction kinetics parameters such as reaction temperature, molar ratio, reaction time. Thus, we selected the direct acylation of **DA** with benzoic anhydride (**BH**) as the synthesis route of **MP**, and put our sight on developing a suitable reactor and revealing reaction intrinsic kinetics to improve reaction selectivity.

The microreactor, also called micro structured reactor or micro channel reactor, has received extensive attention as an efficient and strong tool for continuous synthesis.^{16–19} With its numerous advantages such as large surface area-to-volume ratios, high mixing efficiency, fast mass and heat transfer rates, inherent safety, and precise control over process parameters, this technology has been widely applied in drug synthesis,^{20–24} organic chemistry methodology,^{25–28} chemical engineering^{29–37} and so on.

For the synthesis of **MP** from **DA**, a kind of competitive, consecutive side reaction, where $A + B \rightarrow C$ (target product) and $C + B \rightarrow S$ (side product), if mixing rate is slower than the rate of the reaction, A and B will react before achieving homogeneity. Local concentrations of B in proximity to C are created, which subsequently react to form higher quantities of side-product S.³⁸ However, microreactors inherently have much smaller molecules diffusion times and achieve mixing much faster than in traditional batch reactors. It has been proved that microreactors are suitable to be applied for improving the selectivity of chemical reactions with consecutive side product, such as Friedel-Crafts monoalkylation,^{39,40} [4+2] cycloaddition reactions,^{41,42} monoalkylation of aliphatic amines⁴³ and so on.

More importantly, microreactors have a lot of advantages for performing kinetics measurements, such as high mixing performance, fast heat and mass transfer and precise control over reaction parameters such as reaction temperature, residence time, minute reagents consumption. They have been used to characterize kinetics at the reaction of aniline and benzoyl chloride,⁴⁴ the reaction of *m*-phenylenediamine and benzoic anhydride,⁴⁵ styrene carbonate synthesis,⁴⁶ Gabapentin synthesis,⁴⁷ glucose dehydration⁴⁸ and so on.

However, the synthesis of **MP** with microreactor technology and its kinetics study have not been explored up to now. The motivation for improving the selectivity of **MP** and investigating its kinetics using the microreactor technology arise from above mentioned unique advantages of microreactors.

In this article, the chemical reaction equation of **MP** synthesis is shown in Fig. 1, **SP** is used to represent the double acylation side product. A microreactor system was developed to study the kinetics of the acylation reaction between **DA** and **BH**. A kinetic model was established, the reaction orders of **DA** and **BH** were determined successively by designing different experiments. Then, the values of reaction rate constants, pre-exponential factors and activation energies of each reaction were acquired. Next, validation experiments showed the calculated data fits well with the experimental data. Finally, through the model simulation, the optimized reaction parameters were found to perform the efficient synthesis of **MP** with high selectivity.

Fig. 1. Chemical reaction equation of the reaction between DA and **BH**.

1. **Materials and methods**
2. **Chemicals**

o-Phenylenediamine (**DA**, 98.5 wt%) and acetonitrile (analytical grade) were purchased from Sinopharm Chemical Reagent Co., Ltd (Shanghai, China); Triethylamine (**TEA**, HPLC grade, 99.5 wt%), Diethylamine (**DEA**, ACS, 99 wt%) and Benzoic anhydride (**BH**, 98.0 wt%) was purchased from Aladdin Industrial (Shanghai, China); All reagents were used without further purification.

Solution A (**DA** + **TEA**): **DA** (2.16 g) and **TEA** (2.02 g) were dissolved in acetonitrile (20 mL);

Solution B (**BH**): **BH** (4.52 g) was dissolved in acetonitrile (20 mL);

Solution C (**DEA**): **DEA** (0.146 g) was dissolved in acetonitrile (20 mL).

Then, the three solutions were replenished to a volume of 100 mL with acetonitrile, respectively.

As the concentration of reactants in the experimental process need to be changed occasionally, the above was just one of the appropriate ratios.

Equipment

The experimental setup for the synthesis of **MP** and determination of reaction kinetics is shown in Fig. 2. Two same T-joint mixer were used to start and terminate the acylation reaction between **DA** and **BH**. The Solution A and Solution B were separately pumped into capillaries (316 stainless steel) by two metering pumps (pump A, pump B, FL2200, Zhejiang Fuli Instrument Co.). Next, the feed streams were preheated to the reaction temperature in enough long (0.2 m) coiled stainless capillaries (316 stainless steel), and mixed in the first T-joint mixer. A stainless delay loop (316 stainless steel) was connected directly to the outlet of the first T-joint mixer. The acylation reaction took place in the delay loop, and the residence time could be controlled precisely by varying the flow rate of the reaction mixture or the length of the delay loop. The two preheat tubes, the first T-joint and delay loop were immersed in a same thermostat-controlled water bath to control a constant reaction temperature. After the controlled residence time, the reaction was quenched online in the second T-joint by Solution C, which was pumped into the microreactor by a metering pump (pump C, LC500P, Hangzhou Jingjing Technology Co.). All the capillaries have an inner diameter of 0.64 mm and an external diameter of 1.59 mm, the diameter of microchannel in the two T-joint mixer is 1.2 mm.

Occasionally, when reaction temperature at 0 °C, the water bath was replaced by alcohol bath. When reaction temperature at 120 °C, water bath was replaced by oil bath, due to the limitation of the solvent boiling point, a back-pressure regulation (SS-K9552FZ-1P-, Beijing xiongchuan Technology Co.) was connected directly to the outlet of the microreactor.

In all experiments, the flow rate of Solution A (Q_A) is equal to the flow rate of Solution B (Q_B), the molar ratio of **DA** and **BH** was controlled by changing their concentrations in Solution A and Solution B. To avoid further dilute reactor effluent for HPLC determine, the flow rate of Solution C (Q_C) was controlled at 2 ~ 40 times of Q_A to dilute reaction solution online.

Fig. 2. The schematic overview of the experimental setup.

Quenching and sample analysis

Different quenching conditions were screened to obtain an accurate measurement result, and the results are shown in Part 1, Supplementary material. Due to the relatively fast reaction rate and “off-line detection”, the simple dilution and cooling for reaction solution will cause a larger error to the sample detection. As a result, **TEA** was used as quenching solution because of its stronger nucleophilicity. The acylation reaction between **DEA** and **BH** is almost instantaneous, then the acylation reaction between **DA** and **BH** was online quenched in the second T-joint.

When the microchemical system reached steady state, samples were collected directly from the outlet of quencher and subsequently measured immediately by HPLC (Ultimate 3000, Thermo Fisher Scientific Co.). To avoid oxidation of amine compounds during long-term storage, the samples were stored in brown glass bottle and refrigerator for less than 2 h before analysis. HPLC Conditions: C18 chromatographic column (10-micron, 4.6 × 250 mm, XB-C18, Shanghai Welch Technology Co.); 50% acetonitrile and 50% ultrapure water as mobile phase; mobile phase flow rate is 1 mL/min; detection wavelength at 254 nm, injection volume is 10 μL. The yield and selectivity were calculated by the following equations:

$$yield = \frac{C_{MP} \times Q_t}{C_{BH0} \times Q_B} \quad (1)$$

$$selectivity = \frac{C_{MP}}{C_{MP} + C_{SP}} \quad (2)$$

Where C_{MP} (mol/mL) is the concentration of main product **MP** in the collected samples; Q_t (mL/min) is total flow rate including Solution A, Solution B and Solution C; C_{BH0} (mol/mL) is the initial concentration of **BH** in the Solution B; Q_B (mL/min) is the flow rate of Solution B; C_{SP} (mol/mL) is the concentration

of side product **SP** in the collected samples. By repeating the reactions 3 times under the same condition, the relative measurement error of the yield decreased to 1%, and the average values were shown in Figures. All concentrate data of reactants and products was obtained by HPLC external standard method.

1. Results and discussion

2. Reaction kinetics analysis and mixing performance in the microchemical system

The pathway of each substance in the reaction network is described in Fig. 3. Main product **MP** is generated by the monoacylation between **DA** and **BH** (main reaction), then side product **SP** is generated by the over acylation reaction between **BH** and **MP** (side reaction). Both of the two reactions generate another by-product benzoic acid, due to the amine groups in **DA** and **MP**, to avoid the acid-base reaction between **DA**, **MP** and benzoic acid, strong alkali **TEA** (1 eq., it was calculated with **DA**) was added to bondage benzoic acid in all experiments.

Because an isothermal kinetic model was established, a batch reaction was conducted to determine the fluctuation range of reaction temperature, which is less than 1 °C, so the batch reaction was considered as an isothermal process (Part 2, Supplementary material). Considering the improved heat transfer performance of microreactor, the micro-reaction was also considered as an isothermal process.

Fig. 3. The pathway of each substance.

In most microreactors, mixing performance is determined by the reactant flow rate because of the passive mixing mechanism. Poor mixing would result in a flow-rate variable conversion of reactant, which results in uncertain kinetic measurements. However, the reactant flow rate cannot be increased excessively, an excessive flow rate would lead to the massive consumption of reactant and a larger tube volume would be needed to finish the reaction.⁴⁹ Thus, it's necessary to determine a suitable flow rate for mixer performance. The conversion of **DA** (x_{DA}) at the same residence time but with different flow rates is showed in Fig. 4. x_{DA} stays the same under this condition, indicating that the external diffusion control is well eliminated. In subsequent tests, all flow rates were controlled at more than $50\mu L/min$ to ensure a sufficient mixer performance.

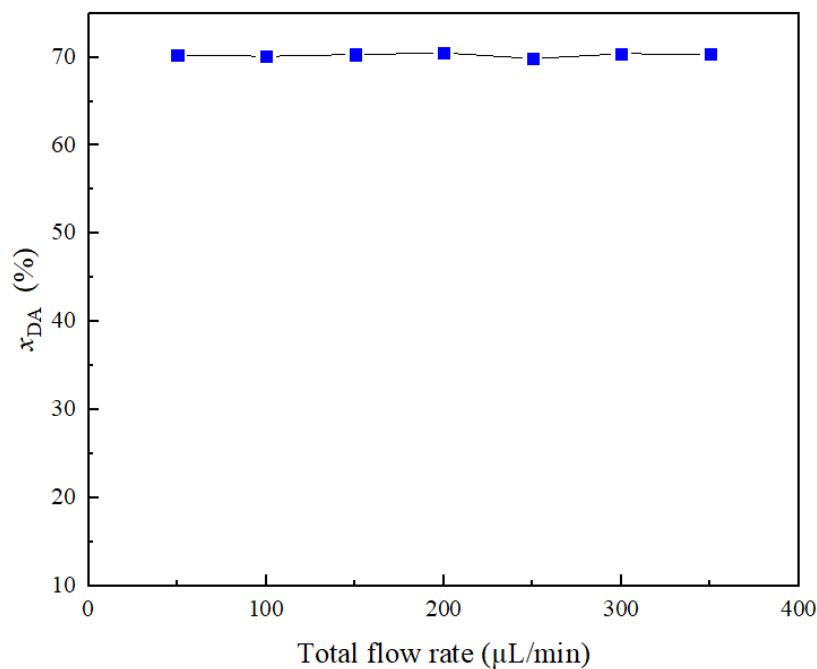


Fig. 4. Conversion of **DA** (x_{DA}) at same residence time with different flow rates. Conditions: reaction temperature (T) = 60 °C; residence time (t) = 271 s; initial concentration of reactants in reaction mixture: **DA** (C_{DA0}) = 0.1 M, **BH** (C_{BH0}) = 0.1 M.

According to Fig. 3 and classic kinetic rules, the kinetic equations are as follows:

$$\frac{dC_{DA}}{dt} = -k_1 C_{DA}^\alpha C_{BH}^\beta \quad (3)$$

$$\frac{dC_{BH}}{dt} = -k_1 C_{DA}^\alpha C_{BH}^\beta - k_2 C_{BH}^\gamma C_{MP}^\delta \quad (4)$$

$$\frac{dC_{MP}}{dt} = k_1 C_{DA}^\alpha C_{BH}^\beta - k_2 C_{BH}^\gamma C_{MP}^\delta \quad (5)$$

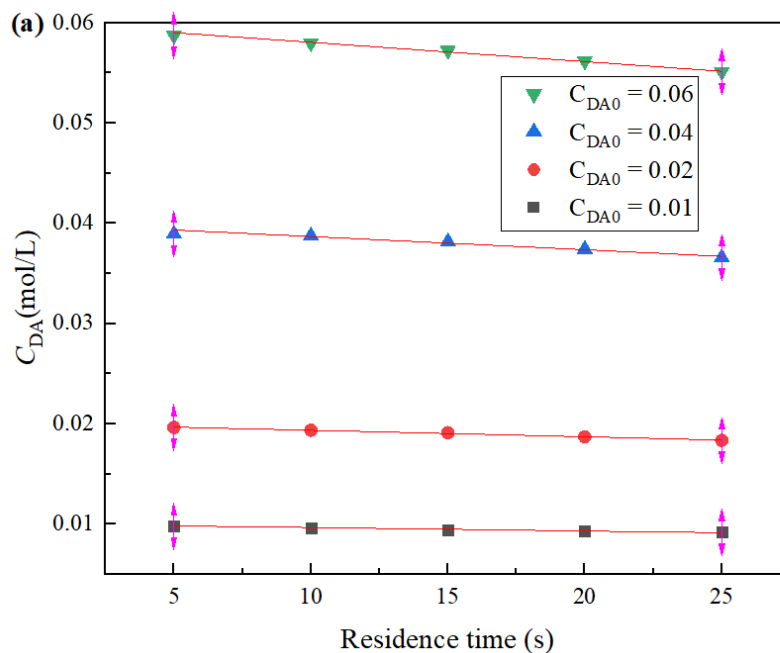
$$\frac{dC_{SP}}{dt} = k_2 C_{BH}^\gamma C_{MP}^\delta \quad (6)$$

α , β , γ and δ stand for reaction orders.

1. Reaction orders

2. The reaction order of *o*-phenylenediamine (DA)

“Initial concentration method” was used to determine the reaction order of **DA**, a set of experiments were carried out on the conditions of different **DA** concentrations, and the results are shown in Fig. 5a. The initial concentration of **BH** was high enough to have influence on the reaction rate. Within the initial 25 s of the reaction, the conversion of **DA** (x_{DA}) less than 9%, consumption of **DA** was negligible, so each plot of concentration versus residence time was a straight line. The slope of each straight line was initial reaction rate of **DA**, as shown in Fig. 5b. The linear relation ($R^2 = 0.999$) between reaction rate and initial concentration of **DA** indicates that this is a first order reaction with respect to **DA**.



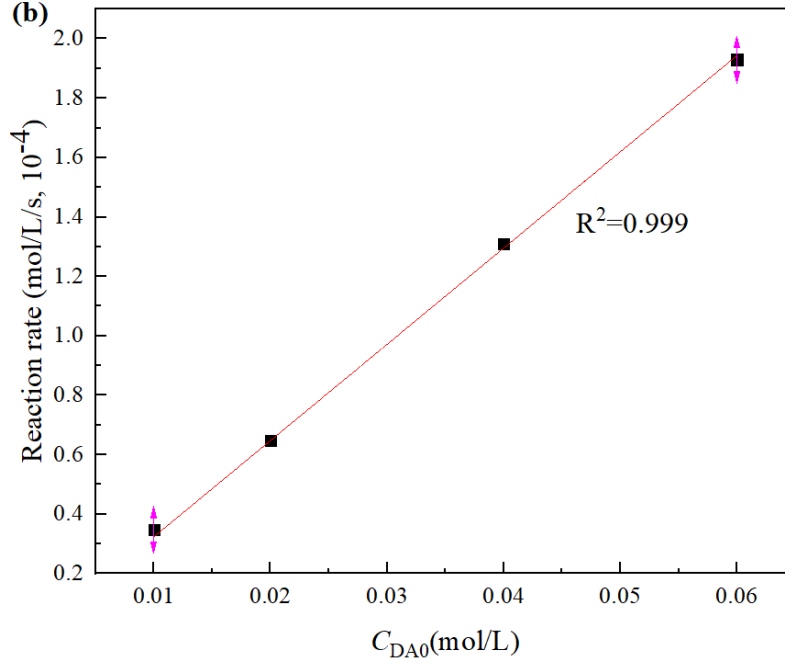


Fig. 5. (a) The concentration changes of **DA** at different initial concentrations of **DA** (C_{DA0}); (b) Reaction rate at different C_{DA0} . Conditions: $T = 40\text{ }^\circ\text{C}$; $C_{BH0} = 0.1\text{ M}$;

The reaction order of benzoic anhydride (BH)

The reaction rate of **BH** (r_{BH}) can be written as:

$$r_{BH} = -k_1 C_{DA} C_{BH}^\beta - k_2 C_{BH}^\gamma C_{MP}^\delta \quad (7)$$

To determine the reaction order of **BH**, the initial concentration of **DA** (C_{DA0}) is 10 times of initial concentration of **BH** (C_{BH0}). Because of excessive **DA**, and the selectivity of **MP** exceeded than 99.5%, so the slight over acylation side reaction can be neglected to simplify the rate law:

$$r_{BH} = -k_1 C_{DA} C_{BH}^\beta - k_2 C_{BH}^\gamma C_{MP}^\delta \approx -k_1 C_{DA} C_{BH}^\beta \approx K_\alpha C_{BH}^\beta \quad (8)$$

If the order of **BH** is first, the rate law is

$$r_{BH} = -\frac{dC_{BH}}{dt} = C_{BH0} \frac{dx_{BH}}{dt} = K_\alpha C_{BH} = K_\alpha C_{BH0} (1 - x_{BH})$$

Where x_{BH} is the conversion rate of **BH**, this equation can be solved by integration as:

$$\ln(1 - x_{BH}) = -K_\alpha t$$

so the plot of $\ln(1 - x_{BH})$ versus t should be a straight line that passes through the origin. Fig. 6(a) and 6(b) show x_{BH} versus t and $\ln(1 - x_{BH})$ versus t respectively. The linear relation $R^2 = 0.998$ in Fig. 6(b) indicates that the reaction order of **BH** in the monoacylation reaction is 1.

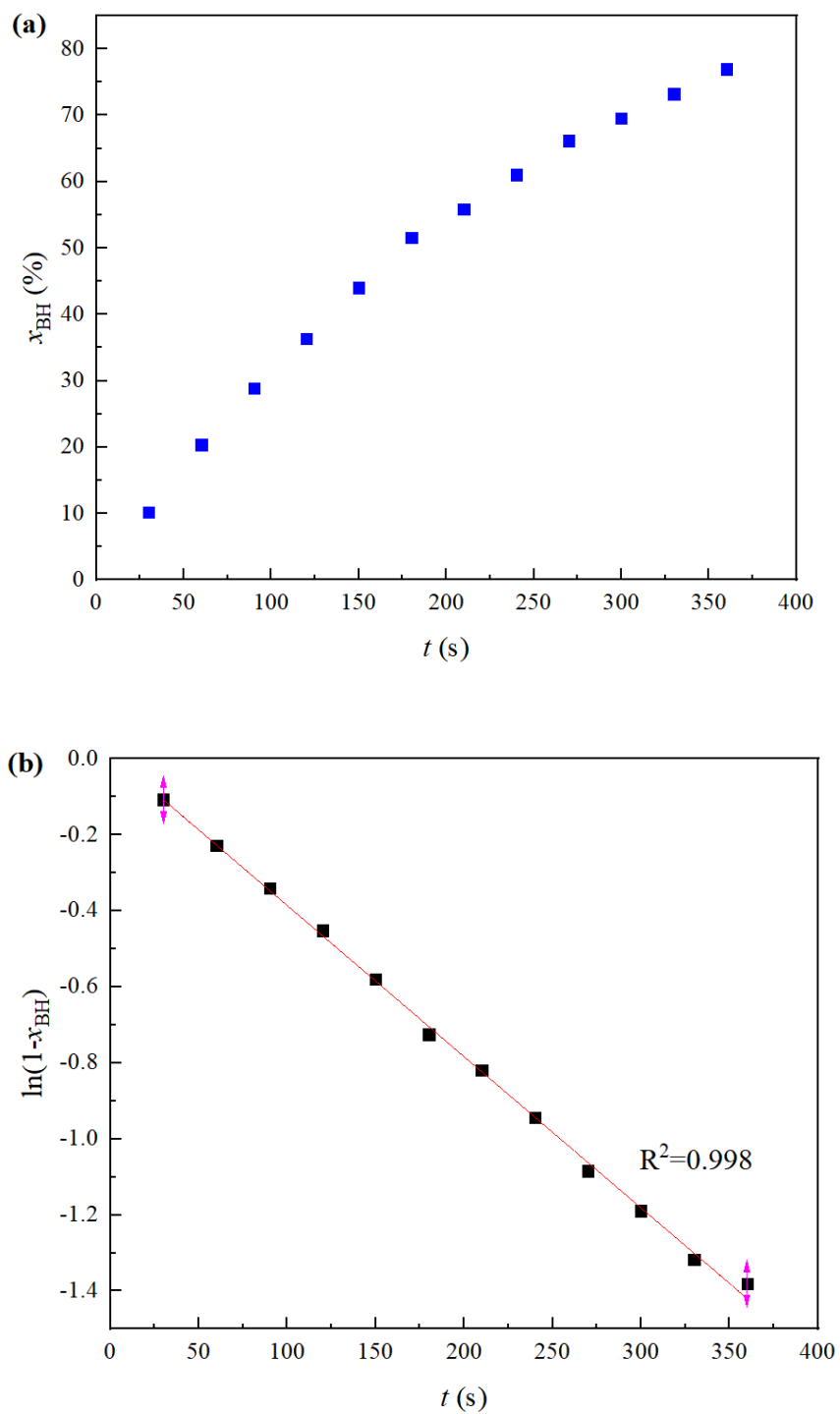


Fig. 6. (a) The conversion rate of **BH**(x_{BH}) versus time (t); (b) $\ln(1-x_{BH})$ versus t . Conditions: $T=40$ °C; $C_{DA0} = 0.1$ M, $C_{BH0} = 0.01$ M;

Since the over acylation reaction and the monoacylation reaction belong to the same type of reaction, the reaction orders in the side reaction are assumed to be 1 ($\gamma = 1$; $\delta = 1$), and total reaction order is 2.

k_1 , k_2 , activation energies and pre-exponential factors

After the reaction orders were determined, the kinetic data was collected at different temperatures and residence times using the microchemical system, and the results are shown in Fig. 7.

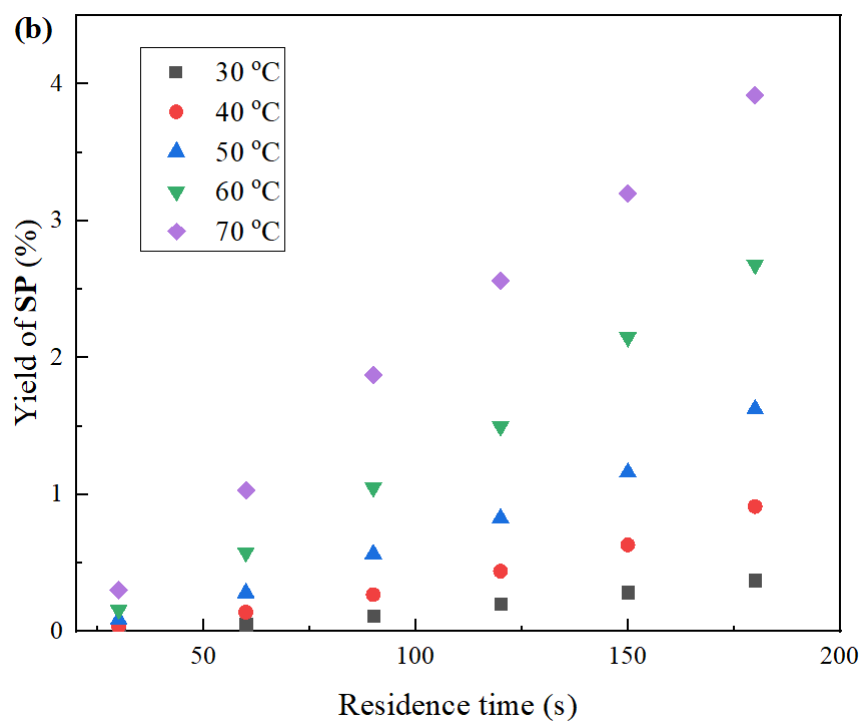
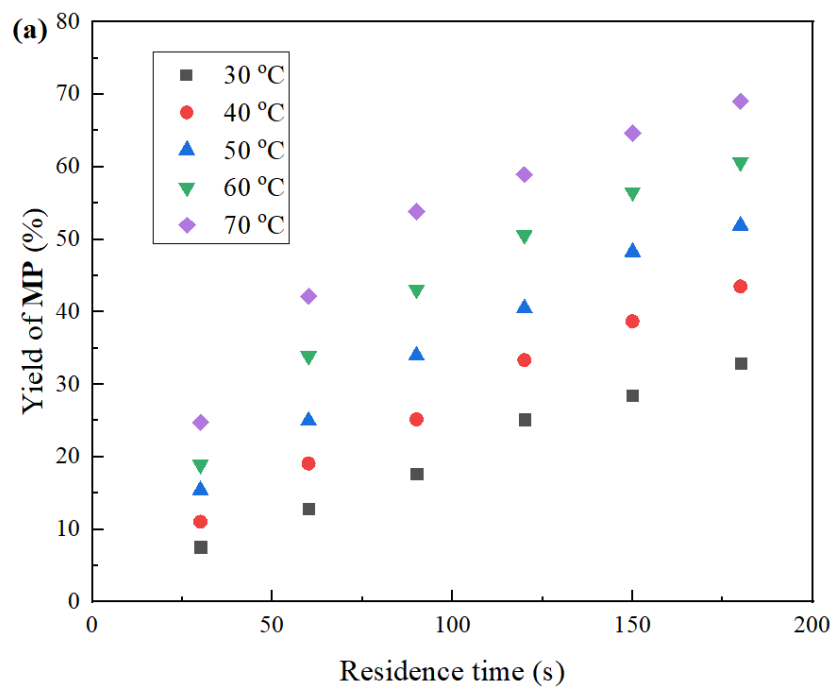
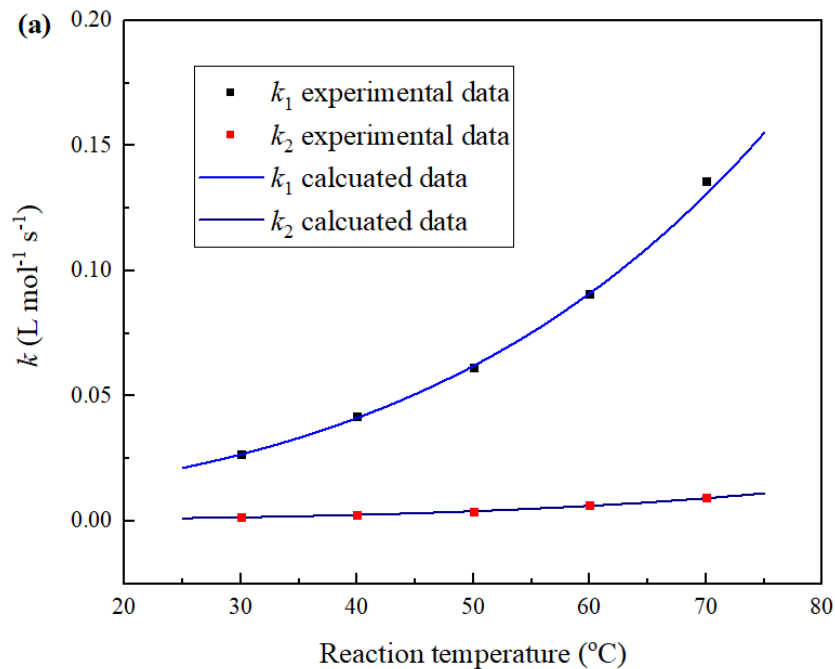


Fig. 7. The yields of **MP** and **SP** at different temperatures and residence times. Conditions: $C_{DA0} = 0.1$ M, $C_{BH0} = 0.1$ M;

The values of k_1 and k_2 at different temperatures were obtained by processing the experimental data in MATLAB software. As shown in Fig. 8(a), the calculated data of k_1 and k_2 fits well with the experimental data at each temperature. After getting k_1 and k_2 at different temperatures, the pre-exponential factors (A_1 and A_2) and activation energies of these two reactions (E_1 and E_2) have been regressed using Arrhenius equation, the results are shown in Fig. 8(b).



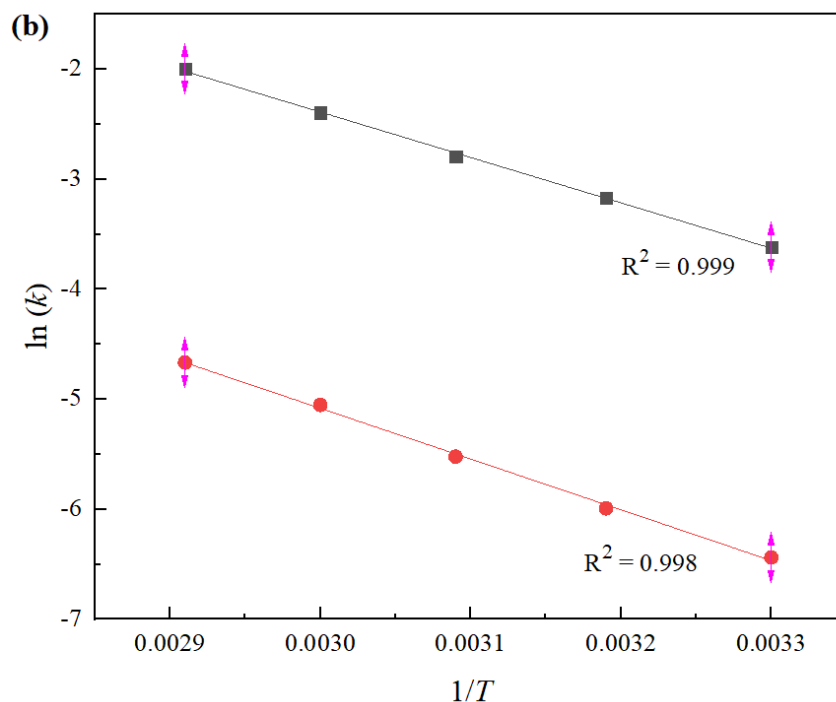


Fig. 8. (a) The experimental and calculated data of k_1 and k_2 . (b) The plot of $\ln(k)$ and $1/T$.

The regression values of k_1 and k_2 are shown in Table 1. The values of pre-exponential factors and activation energies are shown in Table 2. The pre-exponential factors and activation energies of the reaction between **DA** and **BH** are first reported as we have known.

Table 1 Values of k_1 and k_2 at different temperatures

Temperature (°C)	30	40	50	60	70
Values of k_1 (L mol ⁻¹ s ⁻¹)	0.0269	0.0421	0.0613	0.0910	0.1357
Values of k_2 (L mol ⁻¹ s ⁻¹)	0.0016	0.0025	0.0040	0.0064	0.0094

Table 2. Values of the pre-exponential factors and activation energies

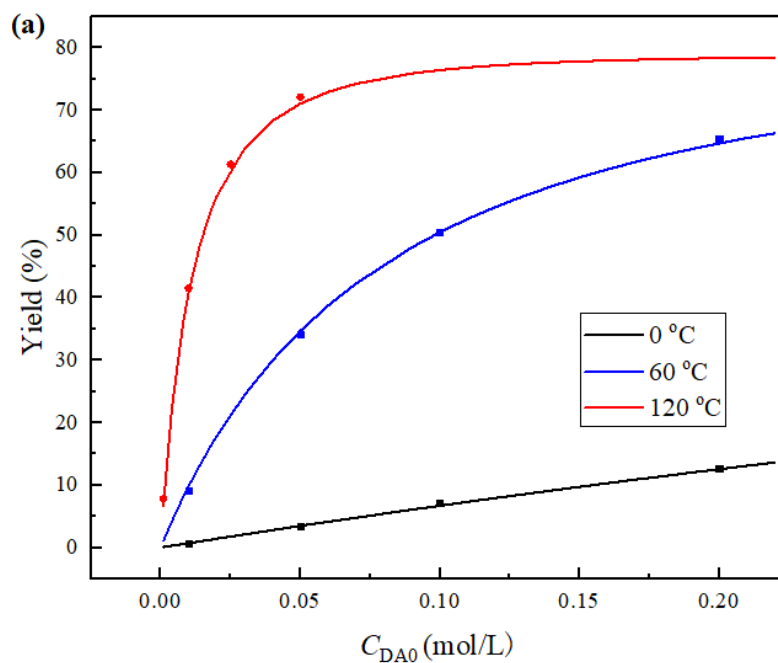
^a

Factors	E_1 (kJ/mol)	A_1 (L mol ⁻¹ s ⁻¹)	E_2 (kJ/mol)	A_2 (L mol ⁻¹ s ⁻¹)
Values	34.30	2.18×10^4	38.36	6.37×10^3

^a E_1 and A_1 are the activation energy and pre-exponential factor in main reaction; E_2 and A_2 are the activation energy and pre-exponential factor in side reaction;

Kinetic model validation

The reaction kinetic model has been verified by changing the reactant concentration and reaction temperature, as shown in Figure 9. The calculated data of yield and selectivity fits well with the experimental data in a large concentration range of 1×10^{-3} - 2×10^{-1} M and a wide temperature range of 0°C - 120°C . When reaction temperature at 120°C , the reacting tube was blocked when the initial concentration at 0.1 M, because the side product **SP** precipitated, so a higher concentration has not been tried. In fact, the solubility of **SP** in many organic solvents is very limited, but the problem will not affect our experiments, since our goal is to develop a flow process with high selectivity. The imperceptible deviations between calculated data and experimental data indicate that the kinetic model is validated. Thus, the reaction kinetic model would be use to optimize the operating conditions.



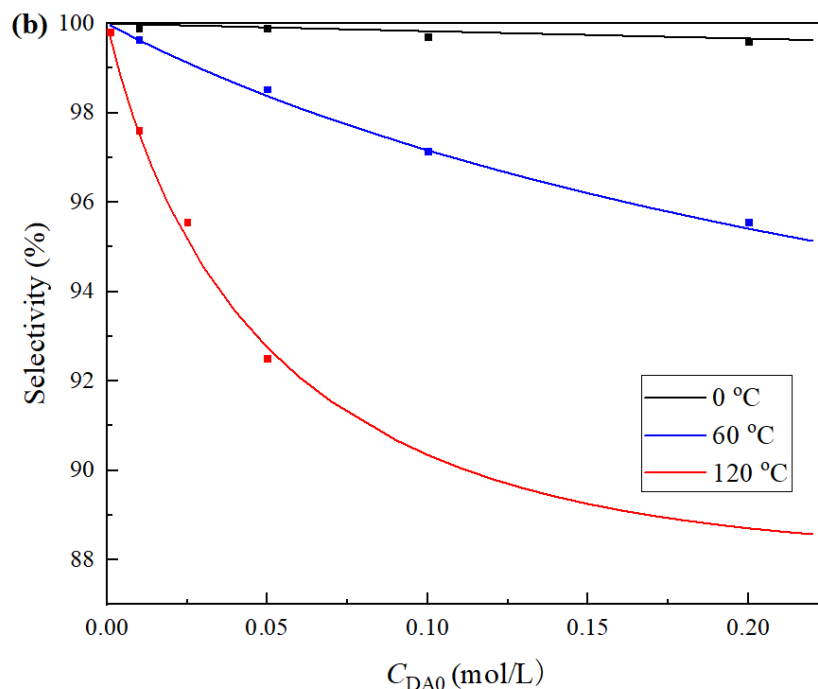


Fig. 9. Kinetic model validation. Lines are calculated data; dots are experimental data. Conditions: $t = 120$ s; molar flow ratio of **DA** and **BH** ($F_{DA}:F_{BH}$) = 1: 1, $C_{DA0} = C_{BH0}$;

1. Reaction parameter optimization through the model simulation
2. Reaction temperature (T)

Obtaining the best yield/selectivity at the shortest residence time and the least material consumption is the most desirable way. As we all know, for this fixed reaction system, the yield was controlled by reaction temperature, molar ratio and residence time. However, the reaction temperature not only affect the target product selectivity but also influence the reaction time (reaction rate). To clearly show this effect, we defined “reaction end time” as the time required for 99.0% conversion rate (the conversion rate was calculated with **BH**). As shown in Fig. 10, with the increasing reaction temperature from 0 to 120 °C, the selectivity just fallen from 92.0% to 88.4%, so the effect of temperature on selectivity is very limited. This is probably because the activation energies of the main reaction and the side reaction are similar, so the effect of reaction temperature on the k_1 and k_2 are similar, thus the change of selectivity is also slight. However, reaction rate enhances sharply with the increasing temperature, such as when reaction temperature at 0 °C, reaction end time is about 10.7 h, but when reaction temperature at 120 °C, reaction end time just needs about 5 min. Hence, the low reaction temperature is not suitable for the synthesis of **MP** because of its slight increase of selectivity but serious recession of reaction efficiency.

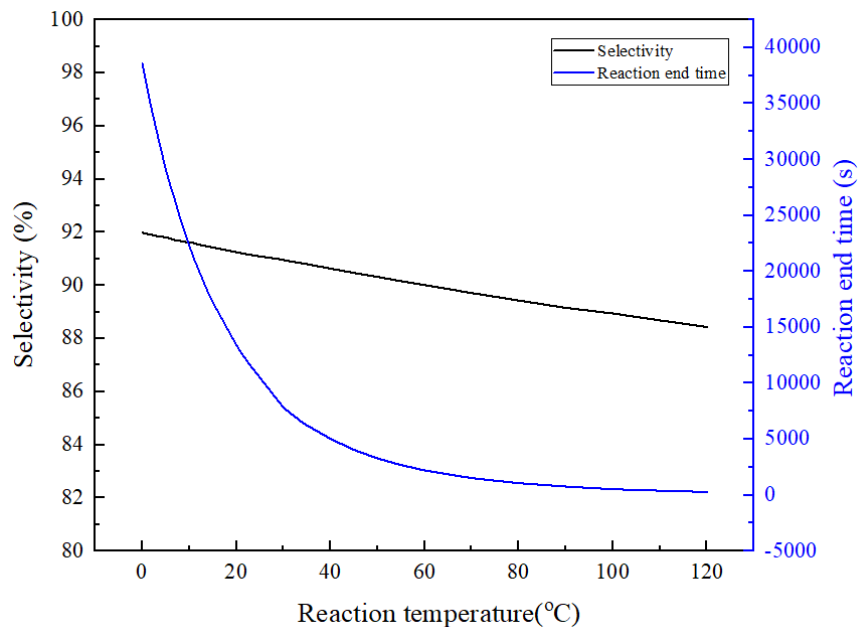


Fig. 10. Simulation results: selectivity and reaction time changes versus reaction temperature. Conditions: $C_{DA0} = C_{BH0} = 0.1$ M; selectivity was calculated under the conversion rate of $BH = 99.0\%$.

The molar ratio of DA and BH ($F_{DA}:F_{BH}$)

The effect of molar ratio between **DA** and **BH** on the selectivity was investigated at temperature 0, 70 and 120°C, and the simulation results are shown in Fig. 11. The selectivity increases continuously with the increasing molar ratio of **DA** and **BH**. Thus, high molar ratio of **DA** and **BH** is requisite to improve reaction selectivity. Moreover, with the increasing the molar ratio, the selectivity difference between different temperature decreases constantly. For instance, at the temperature range of 0 to 120 °C, when molar ratio is 1, the selectivity difference more than 3.5%, when the molar ratio is 2, all the selectivity is greater than 97.0%, and the selectivity difference less than 1.2%. Thus, in the subsequent research, the molar ratio was controlled at 2 to remain a high selectivity.

Fig. 11. Simulation results: the selectivity changes versus molar ratio. selectivity was calculated under the conversion rate of $BH = 99.0\%$.

3.5.3 Residence time (t)

Residence time is an important reaction parameter for process optimization. To understand the reaction process under different residence time, the changes of each substance concentration of different time span at 70 °C and 120 °C are shown in Fig. 12. Amid rising residence time, the yield of **MP** is increasing continuously, and the selectivity remains more than 97.0%. As shown in Fig. 12(a), in the initial 100 s, the yield increased sharply then improved slowly, in the end almost remained constant after 250 s. Because in later period of reaction, since the reactant concentration decreases, the reaction rate become very slow. Therefore, in order to avoid unnecessary time-consuming and improve process efficiency, it's necessary to control an appropriate residence time.

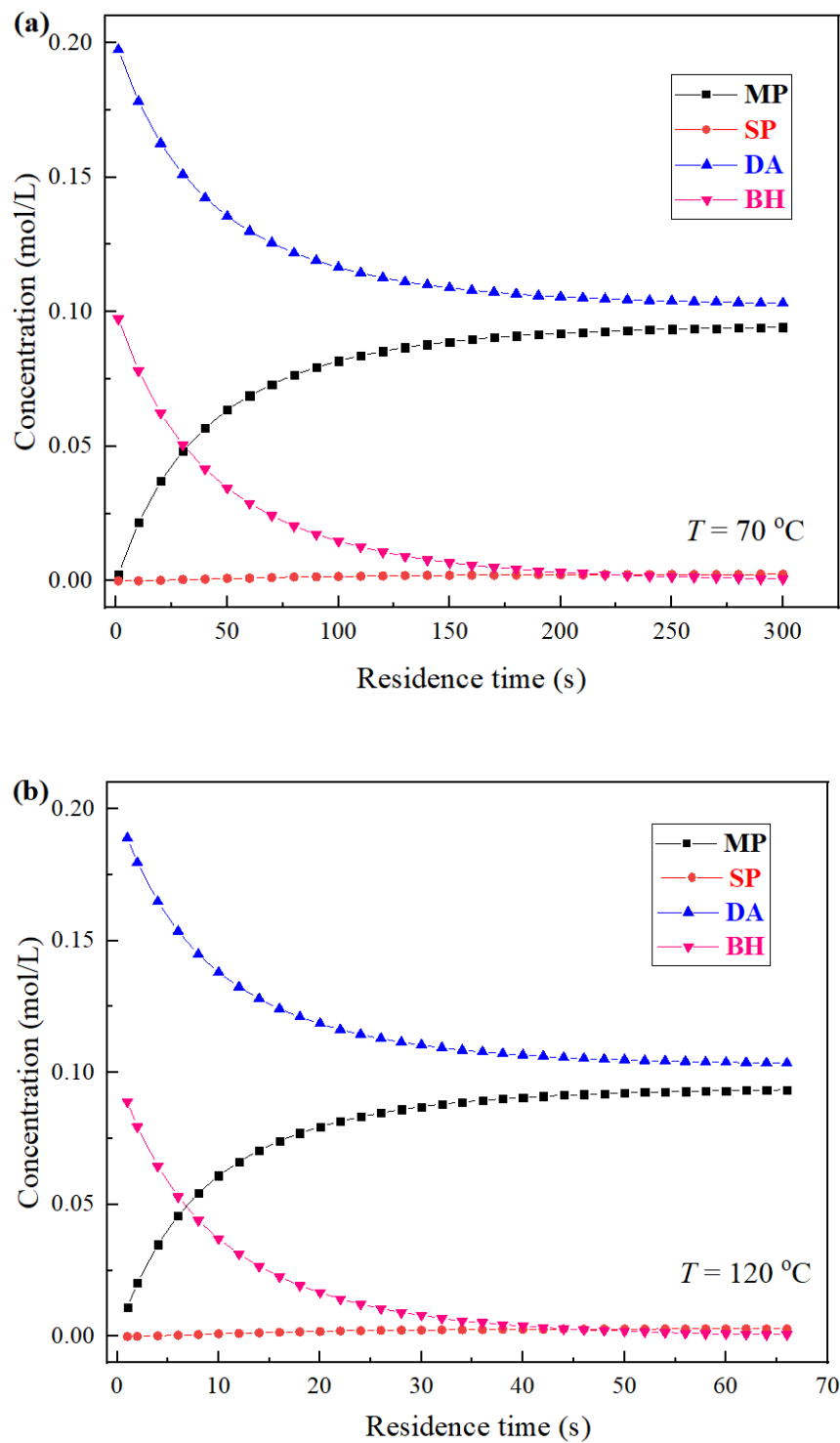


Fig. 12. Simulation results: the concentration of each substance changes versus residence time at $70\text{ }^{\circ}\text{C}$ (a) and $120\text{ }^{\circ}\text{C}$ (b). Conditions: $C_{DA0} = 0.2\text{ M}$, $C_{BH0} = 0.1\text{ M}$.

In the end, we calculated the residence time that satisfies “BH conversion = 99.0%”, which is 275 s for

70°C, and 62 s for 120 °C. Then, the corresponding experiments were conducted, and the experimental results are shown in Table 3, the corresponding calculated data was shown in brackets, which is similar to the experimental data. At two sets of different reaction temperature/residence time, more than 92.0% yield and 96.5% selectivity were obtained in experiments.

Table 3 The results under the optimized condition calculated by the model^a

Reaction temperature (°C)	70	120
Residence time (s)	275	62
Conversion ^b (%)	98.9 ^c (99.0 ^d)	98.5 (99.0)
Yield ^e (%)	92.9 (94.2)	92.1 (93.3)
Selectivity (%)	97.1 (97.5)	96.6 (97.0)

^a Conditions: $C_{DA0} = 0.2$ M, $C_{BH0} = 0.1$ M; ^b the conversion of **BH**; ^c the experiment data;

^d the corresponding calculation data are shown in brackets; ^e the yield of **MP**, it was calculated with **BH**.

Conclusion

In summary, a continuous flow microfluidic system has been developed for the **MP** synthesis with high selectivity. **DA** and simply acylation reagent **BH** were selected as starting material, and the reaction network including a consecutive side reaction. To obtain a controlled selectivity, a kinetic model was established, and detail intrinsic kinetics has been investigated. From the results of kinetic study, the reaction order of **DA** and **BH** in monoacylation reaction both is 1. Then, the values of kinetic constants, pre-exponential factors and activation energies were determined. The kinetic model suggests that high reaction temperature and molar ratio of **DA** with **BH** are necessary to improve reaction rate and inhibit the consecutive side reaction, the appropriate residence time was calculated to improve process efficiency. In the end, all optimization conditions calculated by the model were obtained, more than 92.0% of yield and 96.5% of selectivity were obtained in corresponding experiments.

Acknowledgements

We are grateful to the Zhejiang Provincial Key R&D Project (No. 2018C03074 & 2020C03006 & 2019-ZJ-JS-03) for financial support.

References

1. Suhonen A, Morgan IS, Nauha E, Helttunen K, Tuononen HM, Nissinen M. Effect of a rigid sulfonamide bond on molecular folding: A case study. *Cryst Growth Des* . 2015;15(6):2602-2608.
2. Suhonen A, Nauha E, Salorinne K, Helttunen K, Nissinen M. Structural analysis of two foldamer-type oligoamides - the effect of hydrogen bonding on solvate formation, crystal structures and molecular conformation. *CrystEngComm* . 2012;14(21):7398-7407.
3. Bao XP, Zhou YH. Synthesis and recognition properties of a class of simple colorimetric anion chemosensors containing OH and CONH groups. *Sensors Actuators B: Chem* . 2010;147(2):434-441.
4. Reddy MD, Blanton AN, Watkins EB. Palladium-catalyzed, *N*-(2-aminophenyl)acetamide-assisted *ortho*-arylation of substituted benzamides: application to the synthesis of Urolithins B, M6, and M7. *J Org Chem* . 2017;82(10):5080-5095.
5. Zhou Y, Liu XT, Xue JX, Liu LL, Liang T, Li W, Yang XY, Hou XB, Fang H. Discovery of peptide boronate derivatives as histone deacetylase and proteasome dual inhibitors for overcoming bortezomib resistance of multiple myeloma. *J Med Chem* . 2020;63(9):4701-4715.

6. Suzuki T, Ota Y, Ri M, Bando M, Gotoh A, et al. Rapid discovery of highly potent and selective inhibitors of histone deacetylase 8 using click chemistry to generate candidate libraries. *J Med Chem* . 2012;55(22):9562-9575.
7. Reddy DN, Ballante F, Chuang T, Pirolli A, Marrocco B, Marshall GR. Design and synthesis of simplified Largazole analogues as isoform-selective Human lysine deacetylase inhibitors. *J Med Chem* . 2016;59(4):1613-1633.
8. Nagaraju LR, Venkataravanappa LR, Mandayam Anandalwar S, Khanum SA. Synthesis, X-ray crystal structure study, hirshfeld surface analysis, and biological activity of *N* -(2-amino-phenyl)-2-methylbenzamide. *J Appl Chem* . 2016;2016(15):1-7.
9. Verma SK, Acharya BN, Kaushik MP. Imidazole-catalyzed monoacylation of symmetrical diamines. *Org Lett* . 2010;12(19):10-13.
10. Verma SK, Ghorpade R, Pratap A, Kaushik MP. CDI-mediated monoacylation of symmetrical diamines and selective acylation of primary amines of unsymmetrical diamines. *Green Chem* . 2012;14(2):326-329.
11. Zhang ZX, Yin ZW, Meanwell NA, Kadow JF, Wang T. Selective monoacylation of symmetrical diamines via prior complexation with Boron. *Org Lett* . 2003;5(19):3399-3402.
12. Hikawa H, Imani M, Suzuki H, Yokoyama Y, Azumaya I. Benzoyl methyl phosphates as efficient reagents in the one-pot tandem approach for the synthesis of 2-phenylbenzimidazoles in water. *RSC Adv* . 2014;4(8):3768-3773.
13. Agha KA, Abo-Dya NE, Ibrahim TS, Abdel-Aal EH, Abdel-Samii ZK. *N* -Acylbenzotriazole: convenient approach for protecting group-free monoacylation of symmetric diamines. *Monatshefte fur Chemie* . 2020;151(4):589-598.
14. Moulat L, Martinez J, Salom-Roig XJ. Efficient monoacylation of symmetrical secondary alkanediamines and synthesis of unsymmetrical diacylated alkanediamines. A new L-proline-based organocatalyst. *Arkivoc* . 2019;2019(6):1-14.
15. Bandgar BP, Pandit SS. Highly rapid and direct synthesis of monoacylated piperazine derivatives from carboxylic acids under mild conditions. *Tetrahedron Lett* . 2003;44(19):3855-3858.
16. Jensen KF. Flow chemistry – microreaction technology comes of age. *AIChE J* . 2017;63(3):858-869.
17. Jähnisch K, Hessel V, Löwe H, Baerns M. Chemistry in microstructured reactors. *Angew Chem Int Ed* . 2004; 43(4); 406-446.
18. Brzozowski M, O'Brien M, Ley SV, Polyzos A. Flow chemistry: Intelligent processing of gas-liquid transformations using a tube-in-tube reactor. *Acc Chem Res* . 2015;48(2):349-362.
19. Britton J, Jamison TF. The assembly and use of continuous flow systems for chemical synthesis. *Nat Protoc* . 2017;12(11):2423-2446.
20. Ziegler RE, Desai BK, Jee JA, Gupton BF, Roper TD, Jamison TF. 7-Step flow synthesis of the HIV integrase inhibitor Dolutegravir. *Angew Chem Int Ed* . 2018;57(24):7181-7185.
21. Snead DR, Jamison TF. A three-minute synthesis and purification of ibuprofen: Pushing the limits of continuous-flow processing. *Angew Chem Int Ed* . 2015;54(3):983-987.
22. Xie Y, Huang GM, Wang YJ, Yan ZG, Wang X, Huang J, Gao MT, Fei WY, Luo GS. Synthesis of piperacillin with low impurity content using a new three-feed membrane dispersion microreactor. *Chem Eng J* . 2020;387:124178-124186.
23. Fu WC, Jamison TF. Modular continuous flow synthesis of imatinib and analogues. *Org Lett* . 2019;21(15):6112-6116.

24. Marsini MA, Buono FG, Lorenz JC, Yang BS, Reeves JT, et al. Development of a concise, scalable synthesis of a CCR1 antagonist utilizing a continuous flow Curtius rearrangement. *Green Chem* . 2017;19(6):1454-1461.
25. Ganiek MA, Ivanova MV, Martin B, Knochel P. Mild homologation of esters through continuous flow chloroacetate Claisen reactions. *Angew Chem Int Ed* . 2018;57(52):17249-17253.
26. Karasawa T, Oriez R, Kumagai N, Shibasaki M. Anti-selective catalytic asymmetric nitroaldol reaction of α -keto esters: intriguing solvent effect, flow reaction, and synthesis of active pharmaceutical ingredients. *J Am Chem Soc* . 2018;140(38):12290-12295.
27. Chen Y, Blakemore DC, Pasau P, Ley SV. Three-component assembly of multiply substituted homoallylic alcohols and amines using a flow chemistry photoreactor. *Org Lett* . 2018;20(20):6569-6572.
28. Kim H, Yonekura Y, Yoshida JI. A catalyst-free amination of functional organolithium reagents by flow chemistry. *Angew Chem Int Ed* . 2018;57(15):4063-4066.
29. Shi H, Nie K, Dong B, Chao LM, Gao FX, Ma MY, Long MQ, Liu ZC. Mixing enhancement *via* a serpentine micromixer for real-time activation of carboxyl. *Chem Eng J* . 2020;392:123642-123652.
30. Hu YP, Dong C, Wang T, Luo GS. Cyclohexanone ammoximation over TS-1 catalyst without organic solvent in a microreaction system. *Chem Eng Sci* . 2018;187:60-66.
31. Lebl R, Murray T, Adamo A, Cantillo D, Kappe CO. Continuous flow synthesis of methyl oximino acetoacetate: Accessing greener purification methods with inline liquid-liquid extraction and membrane separation technology. *ACS Sustain Chem Eng* . 2019;7:2008-20096
32. Zha L, Shang MJ, Qiu M, Zhang H, Su YH. Process intensification of mixing and chemical modification for polymer solutions in microreactors based on gas-liquid two-phase flow. *Chem Eng Sci* . 2019;195:62-73.
33. Yu ZQ, Ye X, Xu QL, Xie XX, Dong H, Su WK. A fully continuous-flow process for the synthesis of *p*-Cresol: Impurity analysis and process optimization. *Org Process Res Dev* . 2017;21(10):1644-1652.
34. Yu ZQ, Lv YM, Yu CM. A continuous kilogram-scale process for the manufacture of *o*-difluorobenzene. *Org Process Res Dev* . 2012;16(10):1669-1672.
35. Yu ZQ, Tong G, Xie XX, Zhou PC, Lv YM, Su WK. Continuous-flow process for the synthesis of 2-ethylphenylhydrazine hydrochloride. *Org Process Res Dev* . 2015;19(7):892-896.
36. Yu ZQ, Lv YM, Yu CM, Su WK. Continuous flow reactor for Balz-Schiemann reaction: A new procedure for the preparation of aromatic fluorides. *Tetrahedron Lett* . 2013;54(10):1261-1263.
37. Yu ZQ, Xu QL, Liu LC, Wu ZK, Huang JJ, Lin JY, Su WK. Dinitration of *o*-toluic acid in continuous-flow : Process optimization and kinetic study. *J Flow Chem* . 2020:429-436.
38. Plutschack MB, Pieber B, Gilmore K, Seeberger PH. The hitchhiker's guide to flow chemistry. *Chem Rev* . 2017;117(18):11796-11893.
39. Yoshida J, Suga S, Nagaki A. Highly selective Friedel-Crafts monoalkylation using micromixing. *Chem Commun* . 2003;(3):354-355.
40. Nagaki A, Togai M, Suga S, Aoki N, Mae K, Yoshida JI. Control of extremely fast competitive consecutive reactions using micromixing. Selective Friedel-Crafts aminoalkylation. *J Am Chem Soc* . 2005;127(33):11666-11675.
41. Suga S, Nagaki A, Tsutsui Y, Yoshida JI. "*N*-acyliminium ion pool" as a heterodiene in [4+2] cycloaddition reaction. *Org Lett* . 2003;5(6):945-947.
42. Suga S, Tsutsui Y, Nagaki A, Yoshida JI. Cycloaddition of "*N*-Acyliminium ion pools" with carbon-carbon multiple bonds. *Bull Chem Soc Jpn* . 2005;78(7):1206-1217.

43. Maurya RA, Hoang H, Kim D. Efficient and continuous monoacylation with superior selectivity of symmetrical diamines in microreactors. *Lab Chip*. 2012;12:65-68.
44. Wang PJ, Wang K, Zhang JS, Luo GS. Kinetic study of reactions of aniline and benzoyl chloride in a microstructured chemical system. *AIChE J* . 2015;61(11):3804-3811.
45. Xu QL, Fan HC, Yao HM, Wang DH, Yu HW, Chen BB, Yu ZQ, Su WK. Understanding monoacylation of symmetrical diamines : A kinetic study of acylation reaction of *m*-phenylenediamine and benzoic anhydride in microreactor. *Chem Eng J* . 2020;398:125584-125593.
46. Rehman A, López Fernández AM, Resul MFMG, Harvey A. Kinetic investigations of styrene carbonate synthesis from styrene oxide and CO₂ using a continuous flow tube-in-tube gas-liquid reactor. *J CO₂ Util* . 2018;24:341-349.
47. Huang JP, Sang FN, Luo GS, Xu JH. Continuous synthesis of Gabapentin with a microreaction system. *Chem Eng Sci* . 2017;173:507-513.
48. Zhang H, Yu ZY, Gu T, Xiang L, Shang MJ, Shen C, Su YH. Continuous synthesis of 5-hydroxymethylfurfural using deep eutectic solvents and its kinetic study in microreactors, *Chem. Eng. J* . 2020;391:123580.
49. Qiu L, Wang K, Zhu S, Lu YC, Luo SG. Kinetics study of acrylic acid polymerization with a microreactor platform. *Chem Eng J* . 2016;284:233-239.